J. Cell. Mol. Med. Vol 8, No 2, 2004 pp. 213-222

Coenzyme Q_{10} inhibits mitochondrial complex-1 down-regulation and nuclear factor-kappa B activation

M. Ebadi *, S. K. Sharma, S. Wanpen, A. Amornpan

Center of Excellence For Neurosciences, University of North Dakota School of Medicine & Health Sciences, Grand Forks, North Dakota, USA

Received: December 15, 2003; Accepted: May 31, 2004

Abstract

We have used control-homozygous weaver mutant, and -heterozygous weaver mutant mice in order to explore the basic molecular mechanism of neurodegeneration and the neuroprotective potential of coenzyme Q_{10}. Homozygous weaver mutant mice exhibited progressive neurodegeneration in the hippocampus, striatum, and cerebellum, and a reduction in the striatal levels of dopamine and coenzyme Qs (Q_9 and Q_{10}) without any significant changes in norepinephrine and serotonin. Mitochondrial complex-1 was down regulated; whereas nuclear factor-kappa B was up regulated in homozygous weaver mutant mice. Rotenone inhibited complex-1, enhanced nuclear factor-kappa B, and caused apoptosis in human dopaminergic (SK-N-SH) neurons; whereas nuclear factor-kappa B antibody suppressed rotenone-induced apoptosis, suggesting that enhancing coenzyme Q_{10} synthesis and suppressing the induction of NF-kappa B, may provide neuroprotection.

Keywords: weaver mutant mice • coenzyme Q_{10} • ubiquinone-NADH oxidoreductase (Complex-1) • NF-kappa B • neurodegeneration • neuroprotection

Introduction

Recent studies have shown that tumor necrosis factor alpha (TNFα), interleukins (IL10 and IL6), and interferon gamma (IFN-γ) are induced following 1-methyl, 4-phenyl, 1, 2, 3, 6-tetrahydropyridine (MPTP) intoxication in C57BL/6 mice, suggesting that cytokines network and inducible nitric oxide synthase (iNOS) may be involved in the development of immune changes accompanying degeneration of the nigrostriatal system [1]. Furthermore, TNFα may contribute to the pathogenesis of sporadic Parkinson's disease (PD) *via* up-regulation of iNOS, which in turn induces the generation of reactive oxygen species (ROS) and apoptosis in the dopaminergic (DA-rgic) neurons. These signaling pathways could lead to the activation of transcriptional factor necrosis factor-kappa B (NF-kappa B), which is activated in affected neurons in PD [2-7].

In a previous study, we have reported that coenzyme Q_{10} provides neuroprotection in PD

* Correspondence to: M. EBADI, Ph.D., FACCP
Professor of Pharmacology, Physiology & Therapeutics,
Professor of Neuroscience, Associate Dean for Research and Program Development, School of Medicine,
Director, Center of Excellence in Neurosciences,
University of North Dakota
Associate Vice President for Health Affairs and Medical Research,
University of North Dakota. Grand Forks, North Dakota, USA
Tel.: (701) 777-2284, Fax: (701) 777-4158
E-mail: mebadi@medicine.nodak.edu

[8]. Recently, we have shown that progressive neurodegeneration in developing weaver mutant mice cause oxidative and nitrative stresses, which are accompanied with enhanced lipid peroxidation, caspase-3 activation, reduction in serine-40 phosphorylation of tyrosine hydroxylase, and increases in the level of endogenous tetrahydroisoquinoline (*e.g.* salsolinol) synthesis in the nigrostriatal DA-ergic neurons [9]. We now propose that one of the several possible molecular mechanisms of neurodegeneration could be through depletion of coenzyme Qs in the brain and an induction of NF-kappa B in homozygous weaver mutant (WM_{homo}) mice. Indeed mitochondrial coenzyme Q_9 and Q_{10} were significantly depleted in aging WM_{homo} mice striatum. Furthermore, progressive neurodegeneration in these animals occurred as a result of significant inhibition of complex-1, and induction of NF-kappa B. Rotenone also induced complex-1 inhibition and enhanced NF-kappa B activation in human dopaminergic (SK-N-SH) neurons as observed in WM_{homo} mice, suggesting that enhancing brain regional coenzyme Q_{10} synthesis and suppressing the induction of NF-kappa B may provide neuroprotection.

Materials and Methods

Chemicals

Cell culture materials including powdered Dulbecco's Modified Eagle Medium (DMEM), fetal bovine serum (FBS), strepto-penicillin, Trypsin, and specific primers for RT-PCR were purchased from GIBCO/BRL Life Technologies (Rockville, MD). First-strand cDNA kit was purchased from Stratagene (La Jolla, CA). Mitochondrial $\Delta\Psi$ fluorochrome, 5,5',6,6'-tetrachloro-1,1',3.3'-tetraethylbenzimidazolo-Carbocyanide iodide, (JC-1), nucleocytoplasmic fluorochromes, 4',6-diamidino-2-phenylindole dihydrochloride (DAPI), ethidium bromide, acridine orange, and FITC-conjugated antimouse IgG were purchased from Molecular Probes (Eugene, Oregon). ApoAlert (Annexin-V) was purchased from Beckton-Dickinson, Palo Alto (CA). All other chemicals including coenzyme Q_{10} were of reagent grade quality and were purchased from Sigma Chemical Company (St. Louis, MO).

Experimental animals

An approval for performing experiments on animals was taken from the local ethical committee. Experimental animals were housed in temperature and humidity controlled rooms with a 12 hr day and night cycle and were provided with commercially prepared chow and water ad-libitum. The animals were acclimated to laboratory conditions for at least 4 days prior to experimentation. Care was also taken to avoid any distress to the animals during the period of experiment. Breeder pairs of $control_{wt}$ C57BJ6, and weaver mutant mice, weighing 25-30 g were purchased from Jackson's Laboratories (Minneapolis, MIN). The detailed description of preparing WM_{homo} and WM_{het} mice is available at web site www.jax.org.Jacmice. The animals were maintained and bred in an air-conditioned animal house facility in hepa-filtered cages with free access to water and lab chow. The zinc, copper, and iron contents in the lab chow were monitored by Atomic absorption spectrophotometer to maintain their adequate supply. We used 45 days old animals in this study. The number of animals used in each experimental group is presented in the figure legends.

Neuronal culture

Human neuroblastoma (SK-N-SH) cell lines were cultured in Dulbecco's modified Eagle's medium (DMEM), supplemented with high glucose, glutamine, 3. 7g/l sodium bicarbonate, and 10% fetal bovine serum (pH 7. 4). The cells were incubated in Forma Scientific CO_2 incubator set at 37^0C with 5% CO_2 and 95% oxygen supply and humidified environment under aseptic conditions. The cells were grown in small T-25 flasks to avoid contamination and were grown for 48 hrs in the above medium to sub confluent state. The cellular monolayer was detached using 0.25% trypsin-EDTA solution for 2 min at 37^0C. Trypsin from detached cells was neutralized with 10% fetal bovine serum and the cells were spun at 1200 rpm for 5 min. The cell pellet was washed thrice with Dulbecco's phosphate buffered saline (d-PBS, pH 7. 4) and stored in -80^0C freezer before analysis. We used between 4^{th} to 5^{th} passages of the fresh culture of SK-N-SH cells. These cells become confluent within 72 hrs. For performing fluorescence microscopic analysis of complex-1, we used the cells within 48 hrs. During this period they remain sub-confluent, form monolayers, and do not overlap (a condition necessary for the microscopic analysis). We repeated these experiments at least 5

times and did not use serum free medium during rotenone treatment. We examined the influence of rotenone on the complex-1 activity to correlate and confirm the functional significance of complex-1 down-regulation in WM_{homo} mice with special reference to PD.

Quantitative Analysis

We considered at least 20% reduction in the relative fluorescence units to be significant in order to determine the level of significance. No further attempt was made to evaluate quantitatively the level of significance. To assess rotenone-induced apoptosis, we counted randomly 100 neurons in each microscopic field under low magnification (10X) using a cell counter. The percentage of neurons exhibiting apoptosis was estimated at least 8 times. The cells exhibiting less than 10% apoptosis were not considered significant.

High Performance Liquid Chromatography (HPLC) of coenzyme Qs

High performance liquid chromatography (HPLC) was performed using ISCO pump and JCL-6000 computer software equipped with U. V detector set at 275 nm spectral wavelength was employed to estimate striatal coenzyme Q_9 and $Q_{10.}$ Coenzyme Q_{10} levels were estimated quantitatively using the computer software and by preparing the overlay chromatograms. The striatal tissue was washed with Dulbecco's phosphate buffered saline (D-PBS), and suspended in 0.5 ml of 25% ethanol. The brain tissue (25 mg) was sonicated for 30 sec at low wattage, and 1 ml of hexane was added. The samples were shaken vigorously in the dark chamber and centrifuged at 14,000 rpm for 20 min at 4^0C. The supernatant was dried in nitrogen environment and the residue was reconstituted in Millipore filtered mobile phase (25% Hexane: 75% Methanol). Ten-µl of filtered sample was injected in HPLC to detect coenzyme Q_9 and Q_{10} levels in the mice striatum. The data was quantitated employing JCL-6000 software.

High Performance Liquid Chromatography (HPLC) of monoamines

High performance liquid chromatography (HPLC) was performed using ISCO pump and JCL-6000 computer software equipped with Bioanalytical electrochemical detector. Various monoamines, including norepinephrine (NE), dopamine (DA), homovalinic acid (HVA), 5-hydroxy-tryptamine (5-HT), and 5-hydroxy-indole acetic acid (5-HIAA) were estimated. The conversion of various monoamines was estimated quantitatively using the computer software and by preparing the overlay chromatograms.

Complex-1 Immunohistology

The animals were anesthetized by injecting 350 mg/kg i.p. Tribromoethane and perfused with 10% formaldehyde in phosphate buffered saline (pH 7.4) at room temp. The brain was isolated and mounted to stubs using cryoMount embedding medium. Eight-µm thick frozen sections were cut using Hacker Bright Micro cryostat. The sections were picked on the polylysine-coated microscopic slides and were exposed to 3% goat serum for 1 hr at room temp to block unspecific binding. They were washed thrice with PBS and exposed to primary antibody (complex-1: 1: 300) for 1 hrs at room temp and washed. The sections were then treated with secondary antibody (FITC-conjugated antimouse IgG, dilution 1:10,000) for 2 hrs. The sections were then washed thrice with PBS and mounted in Aqua Mount with photo bleach inhibitor. The fluorescence images were captured using SpotLite digital camera and Image-Pro software. Target accentuation and background inhibition software were utilized to improve the quality of images.

Immunoblotting

For immunoblotting, 10 ml of cell lysate was used for microplate protein determination using Bio-Rad protein assay kit, in 1:4 dilutions of the concentrated dye and bovine serum albumin (Ranging from 0.625 ng–20 mg) as a standard. The micro titer plates were read using micro plate reader at 600 nm spectral wavelength. Cell lysates containing 15 µg of protein were subjected to 12% SDS-poly-acrylamide gel electrophoresis. Proteins were transferred on to nitrocellulose paper by electroblotting using 50 mA current-strength for 1.5 hrs, and transfer efficiency was checked by Ponceau red stain. The blots were incubated overnight in 5% nonfat milk for nonspecific binding, washed thrice in PBS (pH 7.4), and subjected to

1:500 dilution of primary antibody to complex-1 (dilution, 1:500) or NF-kappa B (dilution, 1:300) for 1 hr, washed thrice with PBS (pH 7. 4), and exposed to 1:10, 000 secondary antibody (HRP-labeled anti Mouse IgG) for 2 hrs, washed thrice. Amersham chemiluminescent kit was used for developing the autoradiograms, which were quantitated using Bio-Rad calibrated GS-800 densitometer.

Reverse-Transcription-Polymerase Chain Reaction (RT-PCR)

RT-PCR was performed using Stratagene first strand cDNA kit to prepare cDNA by using murine leukemia virus reverse transcriptase as per manufacturer's instructions, and retinoic acid receptor, glyceraldehydes dehydrogenase (GAPDH), mitochondrial genome encoding complex-1 region (ND-1), and NF-kappa B were amplified using specific primer sequences obtained from the Gene Bank by employing appropriate denaturing, annealing and polymerization thermal cycles protocols. (Primer sequences: NF-kappa B Forward: 5'-CATGCAACAGAGGGGACTTTCCGAGAGG-3', reverse: 5'-CATGCCTCTCGGAAAGTCCCCTCTGTTG-3'; Retinoic Acid receptor gene: Forward: 5'-GGTACCGCGATCCAGAAGCCCTTC-3', Reverse: GGTACCGTACCTGCTGTCCCCTT-3'; Mitochondrial Genome (ND-1 loop encoding ubiquinone NADH oxidoreductase; complex-1): Forward: 5'-CCT-CCC-ATT-CAT-TAT-CGC-CGC-CCT-TGC-3' Reverse: 5'-GAT-GGG-GCC-GGT-AGG-TCG-ATA-AAG-GAG-3' GAPDH 5'-TTCAACGGCACAGTCAAGG-3', Reverse: 5'-CATGGACTGTGGTCATGAG-3' as described in our recent report [10]. The genes were amplified using Brinkmann-Eppendorf Gradient Thermal Cycler. The mRNA was reverse-transcribed using murine leukemia viral reverse transcriptase (MMLV-RT). Taq-DNA polymerase (2. 5U/0.5 μl) was used to amplify genes using specific primer sets and thermal cycles of denaturation, annealing, and polymerization. The amplified products of different molecular weights were resolved simultaneously using 1% agarose gel (GIBCO-BRL) and visualized using Gel documentation system equipped with video camera, UV illuminator, and digital Sony printer. The amplified bands were semi-quantitated using calibrated Bio-Rad (GS-800) densitometer taking GAPDH as a housekeeping gene for normalizing the data.

Digital Fluorescence Imaging Microscopy

The SK-N-SH cells were grown on glass cover slips or multi-chambered microscopic slides, maintained in DMEM, supplemented with 10% fetal bovine serum. The cells were grown for 48 hrs to sub-confluent stage, and were exposed to rotenone (100 nM) and/or Coenzyme Q_{10} (10 μM) overnight. Following incubation they were washed thrice in D-PBS and incubated at 37^0C for 30 min to stain with the mitochondrial marker, JC-1 (5 nM), and stained for 20 min in 10 μg/ml of ApoAlert (Annexin-V), or FITC-conjugated complex-1 antibody and counter-stained with DAPI and propidium iodide, washed thrice with Dulbecco's PBS, mounted on microscopic slides using aqua mount supplemented with a photo-bleach inhibitor, and observed under digital fluorescence microscope (Leeds Instruments, CO, Minneapolis, MN) set at three (blue for DAPI, green for acridine orange or fluorescein isothiocyanate (FITC), and red for propidium iodide or JC-1) spectral wavelengths. The fluorescence images were captured using SpotLite digital camera and Image-Pro software. Target accentuation and background inhibition software were utilized to improve the quality of images. The images were merged to estimate phosphatidyl serine externalization and mitochondrial vs nuclear apoptosis simultaneously.

Statistical Analysis

Repeated measures analysis of variance (Repeated-ANOVA) was employed for the statistical evaluation of the experimental data using Sigma-Stat (version 2. 03). The number of observations made in each experiment group, are presented in the figure legends. Values of $p<0.05$ were considered statistically significant.

Results

Animals

WM_{homo} mice exhibited 40% mortality at the time of birth. Those who survived had reduced life span. Within first 7 days, we did not see any sign of uncoordinated muscular activity and body tremors in these animals. Body tremors and uncoordinated movements were observed during 14

Fig. 1 Gross CNS morphology of $control_{wt}$ (left), WM_{homo} (middle) and WM_{hetro} mice, illustrating swelling and asymmetrical appearance in WM_{homo} mice. Images of the CNS were captured by Hewlett Packard digital camera and processed by Dell computer employing Hewlett Packard Digital Imaging software.

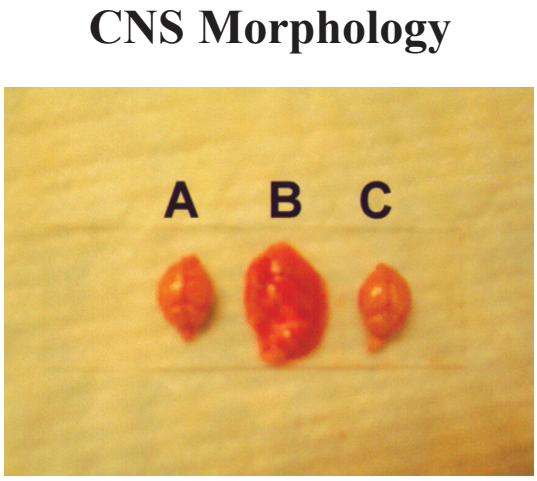

and 28 days. At 45 days they exhibited typical body tremors, drooping body posture, and uncoordinated body movements. Coenzyme Q_{10} treatment for 7 days ameliorated severe body tremors and reduced uncoordinated movements. These symptoms reappeared if coenzyme Q_{10} treatment was withdrawn within 1 month, indicating that a prolonged treatment of coenzyme Q_{10} is required for neuroprotection.

Age and number of animals

Eight animals from control, WM_{homo}, and WM_{hetro} groups were used in this study. Experiments were performed on 45 days old animals. Striatal tissue was used for the CNS examination, HPLC, immunohistology, immunoblotting, and RT-PCR analysis.

Body weight

There was no significant difference in the body weights between $control_{wt}$ and WM_{het} mice. Body weights of 45 days old $control_{wt}$, WM_{homo}, and WM_{het} mice were 30±4g, 18±5 and 28±6 g respectively. Body weight was significantly ($p<0.01$) reduced in WM_{homo} mice when compared with $control_{wt}$ and WM_{het} mice.

Gross CNS morphology

The CNS of homozygous weaver mutant mice was soft, swollen, and exhibited asymmetrical appearance due to accumulation of fluid surrounding the striatal tissue as illustrated in Fig. 1.

Striatal monoamines and their metabolites

Striatal monoamines and their metabolites such as dopamine, dihydroxy phenylacetic acid (DOPAC) and homovalinic acid (HVA) were significantly ($p <0.05$) reduced in WM_{homo} mice as compared to $control_{wt}$ and WM_{het} mice as presented in Table 1. Norepinephrine (NE), 5-hydroxy tryptamine (5-HT), and 5-hydroxyl indole acetic acid (5-HIAA) concentrations were not significantly affected among all the experimental groups studied.

Striatal coenzyme Qs

We have determined primarily coenzyme Q_9 and Q_{10} from the striatal regions of $control_{wt}$, WM_{homo} and WM_{het} mice because of their natural abundance. Coenzyme Q_9 levels were almost twice as high as coenzyme Q_{10}. There was no significant difference in the striatal coenzyme Qs between $control_{wt}$ and WM_{het} mice. However, striatal coenzyme Qs were

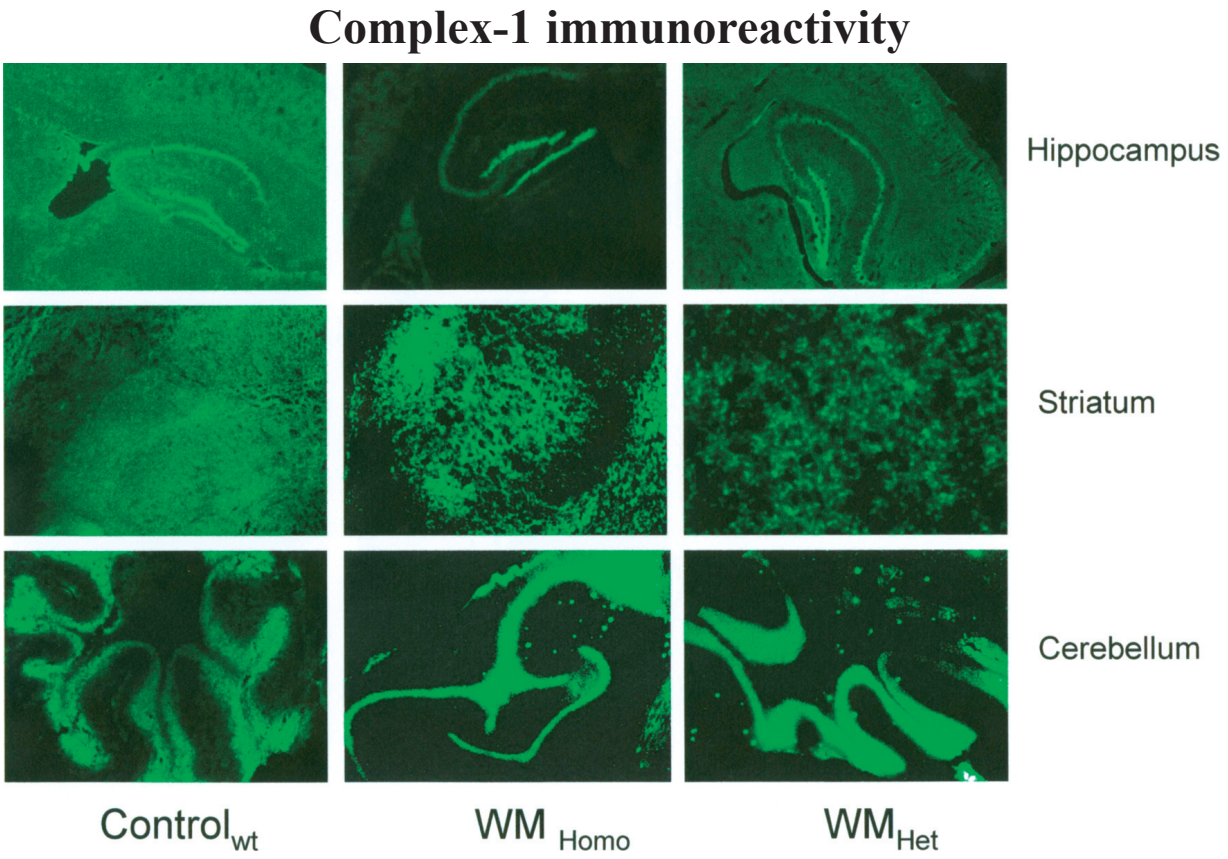

Fig. 2 Representative immunofluorescence microscopic images demonstrating no significant changes in the control$_{wt}$ and WM$_{het}$ mice and a significant reduction complex-1 immunoreactivity in the WM$_{homo}$ mice hippocampus, striatum and cerebellar cortex. Digital fluorescence images were captured by *SpotLite* digital camera and processed by *ImagePro* computer software. (These experiments were repeated 5 times).

Table 1. Striatal Monoamine, their Metabolites, and Ceonzyme Qs.

	Control$_{wt}$	**WM$_{Homo}$**	**WM$_{Het}$**
NE	250±7	200±9	215±10
Dopamine	1850±15	300±10*	1710±9
DOPAC	850±12	150±9	440±14
HVA	150±5	120±7	135±9
5-HT	180±8	175±9	170±6
5-HIAA	90±5	85±7	95±5
Coenzyme Q$_9$	150±7	30±8*	135±6
Coenzyme Q$_{10}$	78±9	20±5**	60±7

Data are Mean±SD of 5-7 determinations for each experimental group and expressed as ng/mg striatal protein. * p <0.05, **p <0.01 (Repeated measures ANOVA). NE: Norepinephrine, DOPAC: Dihydroxy phenyl acetic acid, HVA: Homovalinic Acid, 5-HT: 5-Hydroxytryptamine, 5-HIAA: 5-Hydroxy Indole Acetic Acid.

significantly ($p<0.01$) reduced in WM$_{homo}$ mice as compared to control$_{wt}$ and WM$_{het}$ mice (Table 1).

Complex-1 Immunohistochemistry

Complex-1 immunoreactivity was significantly reduced in the hippocampal, striatal, and cerebellar regions of WM$_{homo}$ mice as compared to control$_{wt}$ and WM$_{het}$ mice. Complex-1 activity was primarily localized in the granular neurons of the hippocampal dentate gyrus and cerebellar cortex. Molecular layers of the hippocampus and the cerebellum exhibited reduced complex-1 immunoreactivity. Complex-1 immunoreactivity was heterogeneously microdistributed in the striatal region and was significantly reduced in the ventral (putamne) regions of WM$_{homo}$ mice when compared with control$_{wt}$ and WM$_{het}$ mice. A maximum reduction in complex-1 was noticed in the striatal region of WM$_{homo}$ mice as compared to control$_{wt}$ and WM$_{het}$ mice as

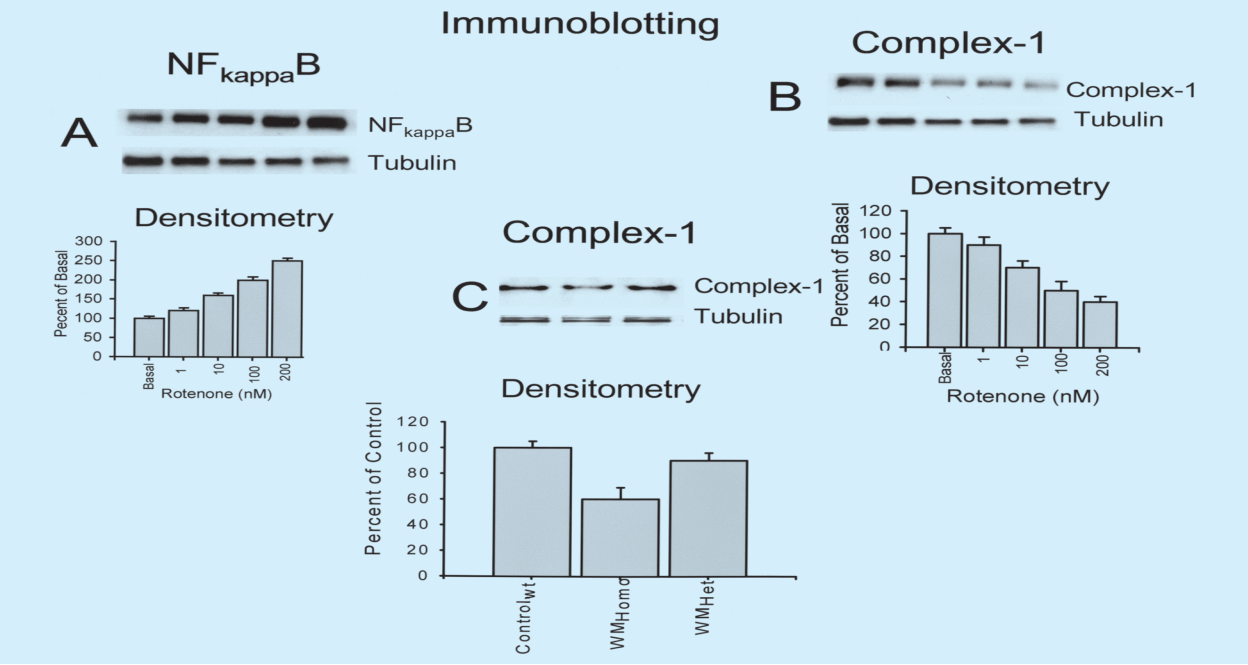

Fig. 3 **A:** Upper left panel; Immunoblots of NF-kappa B and Tubulin in response to increasing concentrations of rotenone in SK-N-SH neurons. Upper left panel: A densitometric analysis to demonstrate concentration-dependent induction of NF-kappa B expression. **B:** upper right panel: Immunoblots demonstrating down-regulation of complex-1 activity in response to increasing concentrations of rotenone. Lower right panel: A densitometric analysis to demonstrate rotenone-induced concentration-dependent down-regulation of complex-1 expression. **C:** Middle panel: Complex-1 activity of $control_{wt}$, WM_{homo}, and WM_{het} mice striatum. Lower middle panel: Densitometric analysis to demonstrate down-regulation of complex-1 expression in WM_{homo} as compared to $control_{wt}$ and WM_{het} mice. Data are Mean±SD of 8 animals *in vivo* experiments and 6-8 experiments on cultured neurons.

illustrated in Fig. 2. Both dorsal (caudate) and ventral (putamen) regions of the striatum exhibited significant reductions in the complex-1 immunoreactivity as determined by digital immunofluorescence imaging microscopy. The ventral striatal region exhibited comparatively more reduction in complex-1 activity as compared to dorsal striatum.

Complex-1 and NF-kappa B Immunoblotting

Rotenone induced concentration-dependent increase in NF-kappa B expression in SK-N-SH neurons as illustrated in Fig. 3, panel A. Rotenone-induced induction in NF-kappa B was associated with complex-1 down-regulation as illustrated in Fig. 3, panel B. A similar kind of complex-1 down-regulation was noticed in aging WM_{homo}-mice (Fig. 3, panel-C).

DNA Fragmentation

Progressive inter-nucleosomal DNA fragmentation was observed in aging WM_{homo} and WM_{het} mice striatum. A slight DNA fragmentation was also noticed in aging $control_{wt}$ mice as well. The DNA fragmentation was significantly high in WM_{homo}, as compared to $control_{wt}$ and WM_{het} mice. A maximum increase in 180-200 base-pair fragment was noticed in aging WM_{homo} mice striatum as presented in Fig. 4A.

Reverse-Transcription Polymerase Chain Reaction (RT-PCR) Analysis

We conducted RT-PCR analysis to determine complex-1 and NF-kappa B mRNA expression in aging $control_{wt}$, WM_{homo}, and WM_{het} mice striatum. Complex-1 mRNA expression was significantly ($p < 0.01$) reduced; whereas, NF-kappa B mRNA expression was signifi-

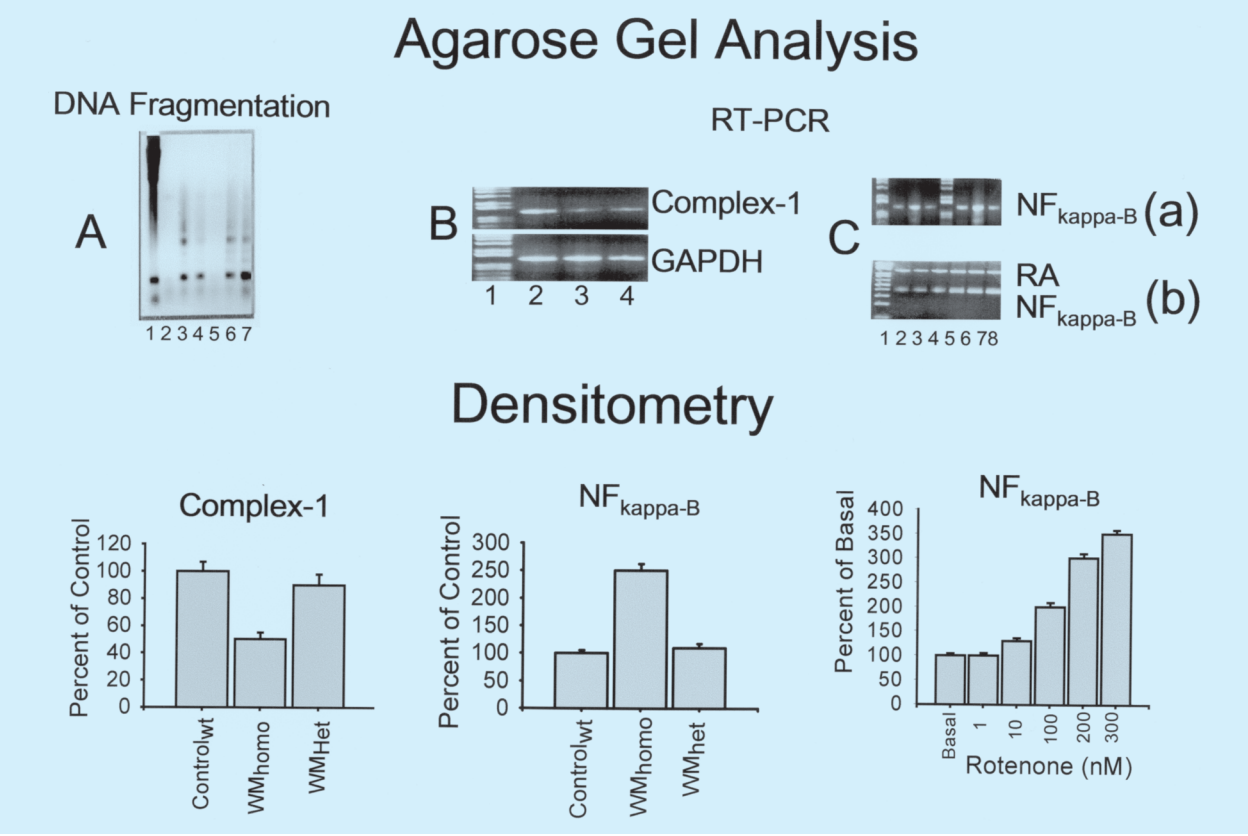

Fig. 4 **A:** Upper left panel: Ethidium bromide-stained 1% Agarose gel analysis of DNA Fragmentation. Lanes 1: 1KDa molecular weight marker, 2, 5: $control_{wt}$, 3, 4:WM_{het}, and 6, 7: WM_{homo} mice striatum demonstrating significantly high DNA damage in the WM_{homo} mice striatum. **B:** Gel analysis of complex-1, and C: $NF_{kappa\text{-}B}$ in mice and SK-NH neurons. Lower panels: Densitometric analysis of complex-1 and $NF_{kappa\text{-}B}$ expression in weaver mutant mice and rotenone-treated SK-N-SH neurons. Data are Mean±SD of 7 animals *in vivo* experiments and 8 experiments on cultured neurons.

cantly ($p<0.01$) increased in WM_{homo} mice as compared to $control_{wt}$ and WM_{het} mice striatum. RT-PCR analysis of complex-1 and NF-kappa B are presented in Fig. 4B and Fig 4C respectively. Densitometric analysis also authenticated quantitative induction of NF-kappa B and inhibition of complex-1 in WM_{homo} mice as compared to WM_{het} and $control_{wt}$ mice. Coenzyme Q_{10} treatment improved complex-1 activity and suppressed NF-kappa B induction in WM_{homo} mice.

NF-kappa-B Expression in SK-N-SH Neurons

We studied complex-1 immunoreactivty in human dopaminergic (SK-N-SH) neurons in response to rotenone. Rotenone induced significant depletion in complex-1 immunoreactivity, down-regulated mitochondrial membrane potential ($\Delta\Psi$), and triggered apoptosis in SK-N-SH neurons as illustrated in Fig. 5. Pre-treatment with coenzyme Q_{10} significantly ($p<0.01$) suppressed rotenone-induced down-regulation of complex-1 and induction of NF-kappa B.

Discussion

Aging $control_{wt}$ (C57BL/6), homozygous weaver mutant (WM_{homo}), and heterozygous weaver mutant (WM_{het}) mice were studied with a primary objective to explore the basic molecular mechanism of neurodegeneration in PD and explore the neuroprotective potential of coenzyme Q_{10}. We have studied the striatal region because it is specifically degenerated in aging weaver mutant mice [11, 12, 13]. Striatal tissue was used for the estimation of monoamines, coenzyme Qs, immunoblotting, and DNA fragmen-

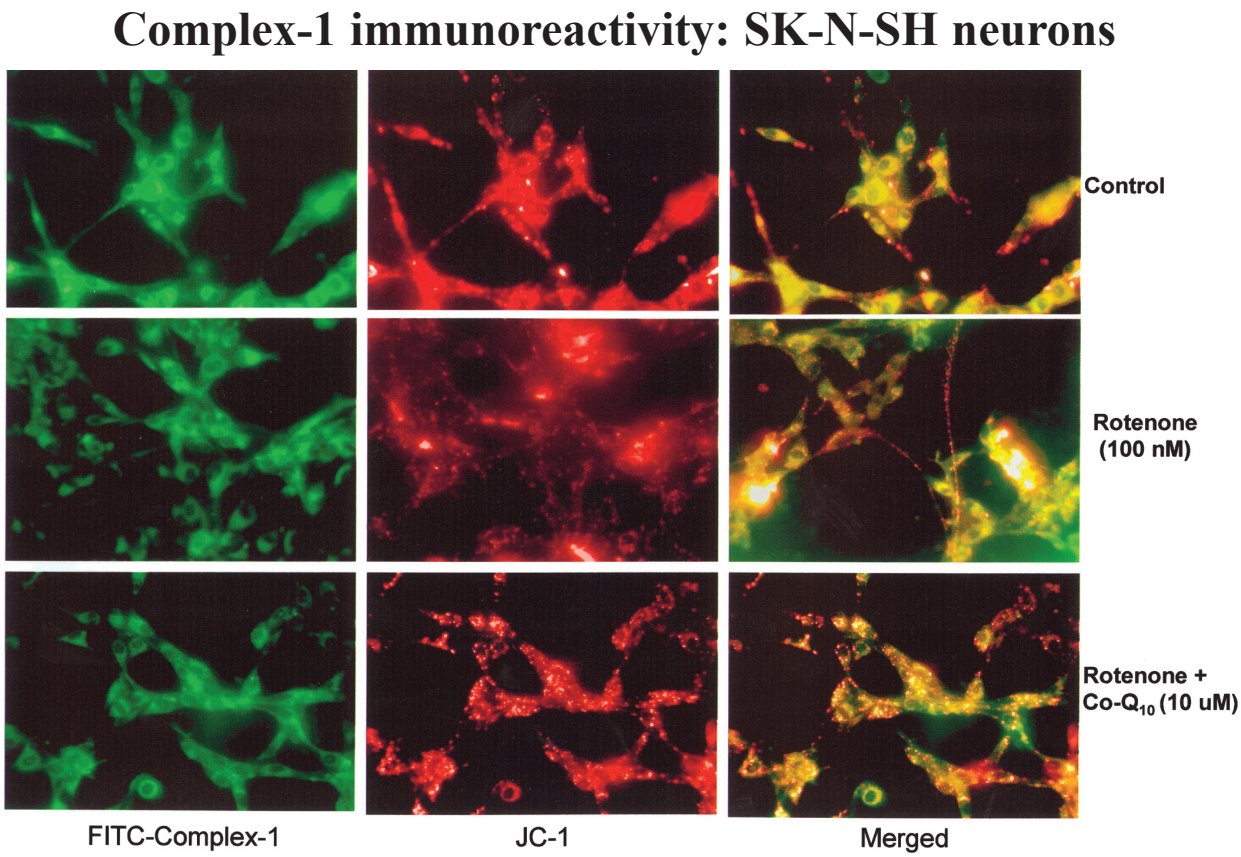

Fig. 5 Complex-1 immunoreactivity (Green) and mitochondrial membrane potential (Red) and merged fluorescence images of SK-N-SH neurons following over night exposure to rotenone and/or coenzyme Q_{10}. Rotenone inhibits mitochondrial complex-1 activity and membrane potential to induce apoptosis in SK-N-SH cells, which was ameliorated upon pre-treating the cells with coenzyme Q_{10}. Digital fluorescence images were captured by *SpotLite* digital camera and processed by *ImagePro* computer software. These experiments were repeated five times.

tation analysis. By employing HPLC-EC, we have demonstrated that DOPAC to DA ratio is significantly altered in WM_{homo} mice when compared with control and WM_{hetro} mice, indicating that impaired DA-ergic neurotransmission might induce progressive neurodegeneration. For the estimation of complex-1 we have employed immunoblotting and immunofluorescence microscopy. We have demonstrated that NF-kappa B is induced and coenzyme Q_{10} synthesis is depleted in WM_{homo} mice CNS. The induction of NF-kappa B and depletion of coenzyme Q_{10} synthesis may contribute to progressive neurodegeneration in WM_{homo} mice. These observations were confirmed in cultured dopaminergic (SK-N-SH) neurons employing rotenone as a specific complex-1 inhibitor. Although the exact molecular mechanism of progressive neurodegeneration in WM_{homo} mice striatum remains unknown, point mutation (glycine156serine) in the pore forming H5 region of GIRK2 channel has been shown to induce hypothyroidism [14], inhibit insulin-like growth factor [15], reduce striatal transforming growth factor-α (TGFα) and dopamine D2 receptor-like immunoreactivity [16], impair synaptic integrity of the neurons in the substantia nigra, and increase caspase-3 activity [17]. These molecular changes affect the basal ganglia circuitry and may be manifested as PD-like movement disorders.

We have performed RT-PCR to establish the transcriptional activation of NF-kappa B and down-regulation of complex-1 in PD. Significant increase in 180-200 bp inter-nucleosomal DNA fragment in our study, suggests active apoptosis in aging WM_{homo} mice. DNA fragmentation might be responsible for neurodegeneration in WM_{homo} mice. However, the exact molecular mechanism of enhanced DNA fragmentation in WM_{homo} mice remains unknown.

Recent studies have suggested an involvement of immuno-modulating factor such as NF-kappa B in the pathogenesis of sporadic PD [17]. The levels of TNFα are also increased in postmortem brain and cerebral spinal fluid from patients with PD. Exposure of TNFα to primary cultures of embryonic rat mesencephalon resulted in a concentration-dependent decrease in DA neurons as evidenced by decrease in the number of TH-immunoreactive cells, suggesting that TNFα mediates cell death in a sensitive population of DA neurons and support the potential involvement of pro-inflammatory cytokines in the degeneration of DA neurons in PD. In conclusion, NF-kappa B is induced whereas complex-1 is down regulated by weaver gene point mutation in WM_{homo} mice and in SK-N-SH neurons in response to rotenone. These early molecular events might trigger DNA fragmentation and apoptosis. Coenzyme Q10 may provide neuroprotection by up-regulating mitochondrial complex-1 and by suppressing NF-kappa B induction.

Acknowledgements

The authors are grateful for the excellent secretarial skills of Kelly Hilzendager for typing this manuscript. These studies were supported by grants from the National Institute of Aging (R01 AG 17059-06 (M. E) and by the Office of National Drug Control Policy # DAT M05-0-C-1252 (M.E.).

References

1. **Ciesielska A., Joniec I., Przybylkowski A., Gromadzdka G., Kurkowska-Jastrzebska I., Czlonkowska A., Czlonkowski A.,** Dynamics of expression of the mRNA for cytokines and inducible nitric oxide synthase in a murine model of the Parkinson's disease. *Acta Neurobiol Exp* (*Wars*) **63:** 117-126, 2003
2. **Wintermeyer P., Riess O., Schols L., Przuntek H., Miterski B., Epplen J.T., Kruger R.,** Mutation analysis and association studies of nuclear factor-kappaB1 in sporadic Parkinson's disease patients. *J. Neurol. Transm* **109:** 1181-1188, 2002
3. **Hirsch E.C., Hunot S.,** Nitric oxide, glial cells and neuronal degeneration in parkinsonism. *Trends Pharmacol. Sci*. **21**: 163-165, 2000
4. **Bringold U., Ghafourifar P., Richter C.,** Peroxynitrite formed by mitochondrial NO synthase promotes mitochondrial Ca^{2+} release. *Free Radical Biol. Med*. **29:** 343-348, 2000
5. **Clarke D.L., Branton R.L.,** A Role for tumor necrosis factor alpha in death of dopaminergic neurons following neural transplantation. *Exp. Neurol*. **176:** 154-162, 2002
6. **Kruger R., Hardt C., Tschentscher F., Jackel S., Kuhn W., Muller T., Werner J., Woitalla D., Berg D., Kuhnl N., Fuchs G.A., Santos E.J., Przuntek H., Epplen JT, Schols L., Riess O.,** Genetic analysis of immunomodulating factors in sporadic Parkinson's disease. *J. Neural Transm*. **107:** 553-562, 2000
7. **McGuire S.O., Ling Z.D., Lipton J.W., Sortwell C.E., Collier T.J., Carvey P.M.**, Tumor necrosis factor alpha is toxic to embryonic mesencephalic dopaminergic neurons. *Exp Neurol*. **169:** 219-230, 2001
8. **Ebadi M., Govitropong P., Sharma S., Muralikrishnan D., Shavali S., Pellet L., Schafer R., Albano C., Josh E.,** Ubiquinone (Coenzyme Q_{10}) and Mitochondria in Oxidative Stress of Parkinson's Disease. *Biological Signals & Receptors.* **10**: 224-253, 2001
9. **Ebadi M., Sharma S., Amornpan A., Maanum S.,** Weaver Mutant Mouse in Progression of Neurodegeneration in Parkinson's Disease. In Parkinson's Disease, Eds M. Ebadi, R. Pfeiffer *CRC Press* (2004).
10. **Sharma S.K., Carlson E.C., Ebadi M.,** Neuroprotective actions of Selegiline inhibiting 1-methyl, 4-phenyl, pyridinium ion (MPP+) -induced apoptosis in SK-N-SH neurons, *J. Neurocytol.,* **32:** 329-343, 2003.
11. **Roffler-Tarlov S., Graybiel A.M.,** The postnatal development of the DA containing innervation of dorsal and ventral striatum: effects of the weaver gene. *J. Neurosci*., **7:** 2364-2372, 1987
12. **Ghetti B., Triarhou L.C.,** Nigrostriatal aberrations induced by weaver gene are present at birth, *Soc. Neurosci. Abstr*., **18:** 156, 1982b
13. **Surmeier D.J., Mermelstein P.G., Goldwitz D.,** The weaver mutation of GIRK-2 results in a loss of inwardly rectifying K^+ current in cerebellar granule cells, *Proc. Natl. Acad. Sci. USA*, **93:** 11191-11195, 1996
14. **Blum M., Weickert C., Carrasco E.,** The weaver GIRK2 mutation leads to decreased levels of serum thyroid hormone: charactrization of the effect on midbrain DA-rgic neuron survival, *Exp Neurol*., **160**: 413-424, 1999
15. **Zhong J., Deng J., Ghetti B., Lee W.H.,** Inhibition of insulin-like growth factor activity contributes to the premature apoptosis of cerebellar granular neurons in weaver mutant mice: *in vitro* analysis, *J. Neuroscience. Res.,* **70**: 36-45, 2002
16. **Xu S.G., Prasad C., Smith D.E.,** Neurons exhibiting DA D2 receptor immunoreactivity in the substantia nigra of the mutant weaver mouse. *Neuroscience,* **89**: 191-207, 1999
17. **Peng J., Wu Z., Wu Y., Hsu M., Stevenson F.F., Boonplueang R., Roffler-Tarlov S.K., Andersen J.K.,** Inhibition of caspases protects cerebellar granular cells of the weaver mouse from apoptosis and improves behavioral phenotype, *J. Biol. Chem.,* **277**:44285-44291, 2002